Optimal Aspect Ratio of Zinc Oxide Nanowires for a Nanocomposite Electrical Generator

K. Momeni[1,*], S.M. Mortazavi Z.[2]

[1] *Department of Aerospace Engineering, Iowa State University, Ames, Iowa 50011, USA*

[2] *Mechanical Engineering-Engineering Mechanics, Michigan Technological University, Houghton, MI 49931, USA*

Abstract

A nanocomposite electrical generator composed of Zinc oxide nanowires (ZnO NWs) was modeled using continuum mechanics and Maxwell's equations. Axial loading was considered and the optimum aspect ratio of ZnO NWs for getting to maximum electric potential was calculated. The bonding between the ZnO NWs and the polymer matrix was considered to be perfect and the linear piezoelectric behavior was assumed. It was shown that the electric potential has maximum and minimum values of opposite signs at the extreme ends along the nanowire length. The maximum generated electric potential varies from 0.01717 for a NW with an aspect ratio of one to 0.61107 for a NW with an aspect ratio of thirty. The optimum aspect ratio of ZnO NW was defined as the difference between the maximum generated electric potential at which the difference becomes less than 1%, which results in an aspect ratio of 16. The results are a major step toward producing ZnO NWs for nanocomposite electrical generators with maximum performance.

Keywords: Nanocomposite Electrical Generators, Zinc Oxide Nanowire, Piezoelectricity

[*] *kmomeni@iastate.edu; Tel: (906) 370 9604*

Introduction

Piezoelectric materials as a new source of energy have been studied over the past two decades.[1-5] Among different piezoelectric materials, ZnO has attracted the attention of the research community.[4, 6] There are some reports on the enhancement of piezoelectricity[4, 6-9] and mechanical[10-11] properties in nanomaterials. The enhancement of piezoelectricity of ZnO nanowires has been demonstrated as nanoscale surface effects.[12] Zinc oxide nanowires have potential applications in nanodevices because of their piezoelectric response.[1, 3-4] Although electric potential generation via bended ZnO NWs has been reported, but the reality of such electric signals is still a matter of debate.[4, 13] Recently, a new approach was introduced for harvesting the electric energy of ZnO NWs, which is based on ZnO NWs embedded in an epoxy matrix[14] and is referred to as nanocomposite electrical generators.[15] Experimental production of nanocomposite electrical generators has been reported.[16] Bended ZnO NWs require special moving devices such as atomic force microscopes for harvesting the generated electric energy, which increases production costs and reduces the device reliability. In contrast, nanocomposite electrical generators are more cost-effective compared to the bended nanowire nanogenerators, and they provide a more stable electric source.

It has been proven that piezoelectric-fiber composites have a higher output voltage-to-applied load ratio than bulk piezoelectric ceramic materials, owing to the large length-to-area ratio of the reinforcing fibers.[17] There are only a limited number of methods for analysis of piezoelectric composites made by embedding piezoelectric fibers into a matrix. The Mori-Tanaka mean field approach[18] and shear-lag model[19] are two more commonly used methods. Mori-Tanaka methods are limited to composites that consists of aligned ellipsoidal inclusions embedded in an epoxy matrix and are not able to capture size-scale effects. This

method also assumes uniform distribution of inhomogenieties.[20] The shear-lag model is applicable for aligned short-fibers and is based on the transfer of tensile stress from matrix to fiber using interfacial shear stress. This model accounts for fiber geometry and can be extended for modeling imperfect surfaces.[21]

The objective of this paper is to find an optimum aspect ratio, L_f/r_o, for ZnO NWs, using the shear-lag model. This would be a major step toward designing new nanocomposite electrical generators with optimum performance. An analytical model for nanocomposite electrical generators was developed using continuum mechanics approach.[19] Solving the derived governing equation[19] of the electric potential for various ZnO NWs with different aspect ratios, it was found that there is an optimum value for the aspect ratio of the ZnO NWs. Based on the presented results, ZnO NWs should have a minimum aspect ratio, L_f/r_o, of 16, so that the generated electric potential may reach to its maximum value at both ends.

Modeling

A single ZnO NW embedded in an epoxy matrix was considered. The representative volume element is shown in Figure 1. The ZnO NW and the epoxy matrix were modeled as elastic isotropic materials. The bond between the ZnO NW and the epoxy matrix is assumed to be perfect, and the ZnO NW was modeled as a cylinder. Although modeling the ZnO NW as an isotropic material might not be the best choice, it simplifies the calculations while representing an acceptable approximation of the reults.[22] Zinc oxide NWs show the maximum reinforcing effect along their longitudinal direction. Therefore, here simple longitudinal tensile loading along the axis of the NW was considered.

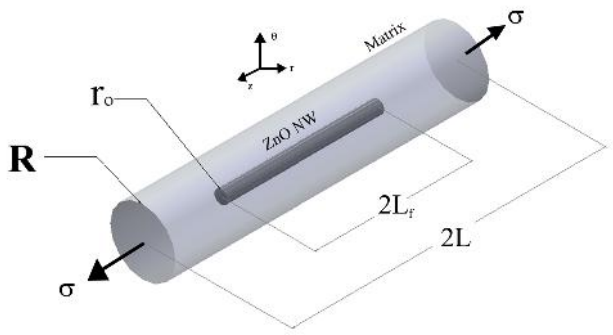

Figure 1. RVE of a ZnO NW with length of $2L_f$, embedded in a matrix with length of 2L. The composite is subjected to the overall stress of σ along the cylindrical axis. R is the outer radius of the RVE and r_o is the radius of the ZnO NW. Reprinted with permission from J. Appl. Phys. 108(11), 114303 (2010). Copyright 2010 American Institute of Physics.[19]

General mechanical and electrical field equations, i.e. conservation of linear momentum and Gauss's law of electric field, were used in combination with constitutive equations to derive the analytical relation between the applied load and potential distribution along the NW. The shear-lag model was used to describe the load transfer between the matrix and the NW.[23] This model has been successfully used for modeling 1D nanostructures.[24-25]

The conservation of linear momentum in the absence of body forces and acceleration is:

$$\nabla \cdot \mathbf{T} = \mathbf{0} \tag{1}$$

where **T** is the stress tensor. Gauss's law in the absence of free charges is:

$$\nabla \cdot \mathbf{D} = \mathbf{0} \tag{2}$$

The mechanical and electrical responses of the ZnO NW, assuming linear piezoelectric behavior, are coupled via the constitutive equations as follows:[26]

$$\begin{cases} \mathbf{T} = \mathbf{c}_E \mathbf{S} - \mathbf{e}^T \mathbf{E} \\ \mathbf{D} = \mathbf{e}\mathbf{S} + \boldsymbol{\kappa}\mathbf{E} \end{cases} \tag{3 a,b}$$

where **S** is strain tensor, **E** is the electric field vector, $\mathbf{c}_E$ is the elastic stiffness tensor, **e** is the piezoelectric constant tensor, © is permittivity tensor, and $\mathbf{e}^T$ is the transpose of the tensor **e**. The electric field vector is related to the electric potential field ¤ via:

$$\mathbf{E} = -\nabla ¤ \tag{4}$$

The constitutive equations (3 a,b) are coupled via the piezoelectric constant tensor. A perturbation technique was used for decoupling the equations, which the details of it was described in the literature.[19, 22]

The 3D problem reduces to a 2D problem in terms of *z* and *r* (Figure 1), due to axisymmetry of geometry and loading. Assuming the radial strain of NW to be much less than its axial strain (i.e. $\varepsilon_{rr} << \varepsilon_{zz}$ for the NW), $R>>r_o$ (low concentration of NWs), and using the shear-lag model, the stress along the ZnO NW in terms of the cylindrical coordinate system is calculated.[25]

The following dimensionless variables are defined:

$$¤^* = ¤ \frac{\left(E_f / \pm\right)}{r_o\, e_{33} / ©_{11}}; \quad r^* = r / r_o; \qquad z^* = z \sim; \quad H = \sim r_o \tag{5}$$

where ± is the applied axial stress and α is a parameter with the dimension of $[L]^{-1}$. The value of α depends on the mechanical and geometrical properties of NW and matrix material.[25] The governing differential equation for electric potential along the NW is[19]

$$\frac{\partial^2 ¤^*}{\partial {r^*}^2} + \frac{1}{r^*}\frac{\partial ¤^*}{\partial r^*} + H^2 \frac{©_{33}}{©_{11}}\frac{\partial^2 ¤^*}{\partial {z^*}^2} = \left(\frac{1}{2}\left(¬_f^2 r^* + \left(¬_f^2 - ¬_f\right) r^* \frac{e_{31}}{e_{33}}\right)\cosh\left(z^*\right) H^2 + \left(1 - ¬_f^2 - \left(¬_f^2 + ¬_f\right)\frac{e_{31}}{e_{33}} - \left(¬_f + 1\right)\frac{e_{15}}{e_{33}}\right)\sinh\left(z^*\right) H\right) B \tag{6}$$

where *B* is defined as follows:

$$B = \left(1 - R^2 \Big/ \left(r_o^2 + \frac{E_m}{E_f}\left(R^2 - r_o^2\right)\right)\right) \Big/ \cosh\left(\sim L_f\right) \quad (7)$$

Equation 6 is a second-order nonhomogeneous partial differential equation with variable coefficients. This type of equation can only be solved using numerical methods. An appropriate numerical method must be chosen that can accurately handle the singularity in equation 6 at the NW axis. Here the governing differential equation was solved for nanowires with different aspect ratios using the numerical technique introduced by Momeni et al.[19]

Case Study

The governing differential equation, i.e. Equation 6, was solved for NWs with aspect ratios varying from one to thirty. The epoxy matrix was assumed to have a Young's modulus of $E_m = 2.41$ GPa and Poisson's ratio of $v_m = 0.35$.[27] To fulfill the assumption of low NW concentration, it was assumed that $R = 5\ r_o$. The dimensions of the ZnO NW were assumed to be the same as those reported in the literature,[22] i.e. the radius of all NWs is $r_o = 25\ nm$. The aspect ratio of NWs, i.e. L_f/r_o, varies from one to thirty.

In this study the elastic modulus of the NW was assumed to be $E_f = 129$GPa.[28] The permittivity of the bulk ZnO is $©_{11} = 7.77©_0$, $©_{22} = ©_{11}$ and $©_{33} = 8.91©_0$, where $©_0$ is the permittivity of a vacuum $©_0 = 8.854\times10^{-12}$ A·s/V·m.[29] The piezoelectric constants are $e_{31} = -0.51\ C/m^2$, $e_{33} = 1.22\ C/m^2$ and $e_{15} = -0.45\ C/m^2$ which has been measured for ZnO films.[30]

The governing differential equations were solved for NWs with aspect ratios varying from one to thirty. Distribution of the electric potential along the axis of nanowires with different aspect ratios is shown in Figure 2(a). It can be seen that the maximum and minimum

generated electric potentials occur at the extreme ends of NWs, which are equal in magnitude but have opposite signs. Furthermore, the maximum dimensionless electric potential increased from 0.01717 for the NW with the aspect ratio of one to 0.61107 for a NW with the aspect ratio of thirty.

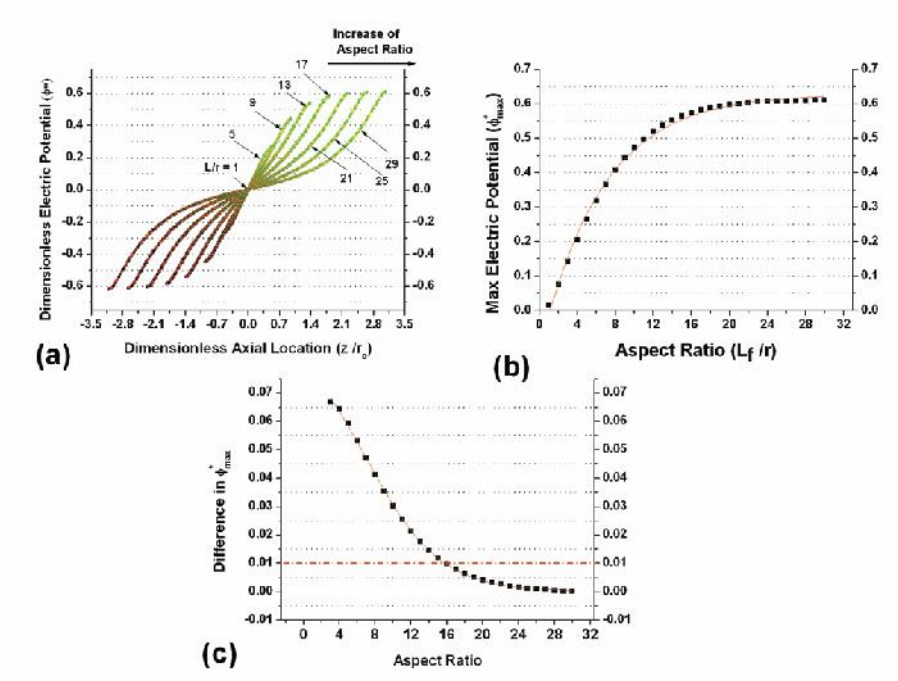

Figure 2. (a) Distribution of electric potential along ZnO NWs with different aspect ratios. (b) Max dimensionless electric potential along the NW for different aspect ratios. (c) Difference in the maximum electric potential of NWs with consecutive aspect ratios. The red dash dot line along the 1% line shows the criteria for specifying the NW with optimum aspect ratio, which is the NW with the aspect ratio of 16. The maximum electric potential increases by increasing the aspect ratio of the NWs, and it reaches to $\phi^* \sim 0.6$.

Maximum dimensionless electric potential as a function of the aspect ratio of NWs is shown in Figure 2(b). Here, the optimum aspect ratio defined for ZnO NWs at the maximum generated electric voltage increases by less than 1%, as the aspect ratio of the NWs increase. The difference in the maximum generated electric potential of the NWs is shown in Figure 2(c). The difference between maximum generated electric potential NWs decreases by increasing the aspect ratio of the NWs. The red dash dot line in this graph shows the criteria of choosing the

optimum aspect ratio of NWs, i.e. dimensionless electric potential increase by less than 1%, which indicates that an aspect ratio of 16 is the optimum aspect ratio.

Dimensionless shear stress, T_{rz}/σ, and dimensionless axial stress, T_{zz}/σ, were distributed along the ZnO NWs with different aspect ratios as shown in Figure 3 using the formulation introduced by Momeni et al.[25]

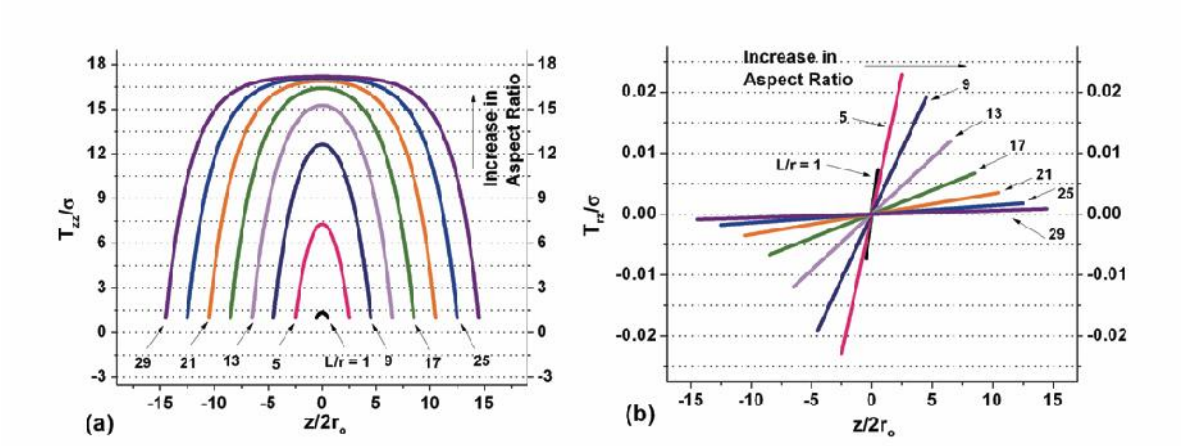

Figure 3. (a) Dimensionless axial stress distributions T_{zz} /±, and (b) Dimensionless shear stress distributions T_{rz} /± along the axis of ZnO NWs of $r_o = 25nm$ and different aspect ratios L_f/r_o ranging from one to thirty, are shown along the axis of NW z / r_o. The maximum shear stress occurs at extreme ends of the nanowire; i.e. ² = ²$_{max}$ at $z = \pm L_f$, while it vanishes at the middle of the NW, T_{rz} /± = 0 at $z = 0$. At the extreme ends the stress that transfers to the end caps is the same magnitude as the applied stress, σ. The model dictates transfer of applied external stress to the NW through the matrix. Moving away from the NW ends, axial stresses increase due to an increase in transferred shear stresses between the matrix and NW, with the maximum at z = 0.

The maximum shear stress occurs at the extreme ends of NWs, and the maximum axial stress occurs at the center. Furthermore, minimum axial stress is equal to the applied external stress, σ, and is at the extreme ends of the NW, while minimum shear stress is zero and occurs at the center of the NW.

Conclusion

An analytical model was used for predicting the generated electric voltage distribution along the zinc oxide nanowires with different aspect ratios, embedded in an epoxy matrix and

subjected to axial stress. It was shown that the electric voltage has its extremum value along its axis at the extreme ends, and is a strong function of distribution of shear stress. The effect of the nanowires aspect ratio on the generated electric voltage has been investigated. It was shown that the optimum aspect ratio for nanowires to generate the maximum electrical potential along their axis is about 16.

The distribution of axial and shear stresses along the ZnO NW were also calculated. While axial stress was maximized in the middle of the NW, the shear stress was maximized at the ends of the NW. Also, the distribution of electric potential was attributed to shear stress transfer at the interface of nanowire and the surrounding polymer matrix.

There are reports about the effect of electro-mechanical boundary conditions on elasticity of zinc oxide nanowires.[31-32] However, in this paper such effects were not considered. The results presented here represent a major step toward designing nanocomposite electrical generators with optimum performance.

References:

1. Gao, P.X., J. Song, J. Liu and Z.L. Wang, *Nanowire Piezoelectric Nanogenerators on Plastic Substrates as Flexible Power Sources for Nanodevices.* Advanced Materials, **19**, 67-72 (2007).
2. Huang, M.H., S. Mao, H. Feick, H. Yan, Y. Wu, H. Kind, E. Weber, R. Russo and P. Yang, *Room-Temperature Ultraviolet Nanowire Nanolasers.* Science, **292**, 1897-1899 (2001).
3. Song, J., J. Zhou and Z.L. Wang, *Piezoelectric and Semiconducting Coupled Power Generating Process of a Single ZnO Belt/Wire. A Technology for Harvesting Electricity from the Environment.* Nano Letters, **6**, 1656-1662 (2006).
4. Wang, Z.L. and J. Song, *Piezoelectric Nanogenerators Based on Zinc Oxide Nanowire Arrays.* Science, **312**, 242-246 (2006).
5. Zhou, J., P. Fei, Y. Gao, Y. Gu, J. Liu, G. Bao and Z.L. Wang, *Mechanical−Electrical Triggers and Sensors Using Piezoelectric Micowires/Nanowires.* Nano Letters, **8**, 2725-2730 (2008).
6. Zhao, M.-H., Z.-L. Wang and S.X. Mao, *Piezoelectric Characterization of Individual Zinc Oxide Nanobelt Probed by Piezoresponse Force Microscope.* Nano Letters, **4**, 587-590 (2004).
7. Xiang, H.J., J. Yang, J.G. Hou and Q. Zhu, *Piezoelectricity in ZnO nanowires: A first-principles study.* Applied Physics Letters, **89**, 223111-3 (2006).
8. Li, C., W. Guo, Y. Kong and H. Gao, *Size-dependent piezoelectricity in zinc oxide nanofilms from first-principles calculations.* Applied Physics Letters, **90**, 033108-3 (2007).

9. Mitrushchenkov, A., R. Linguerri and G. Chambaud, *Piezoelectric Properties of AlN, ZnO, and HgxZn1−xO Nanowires by First-Principles Calculations.* The Journal of Physical Chemistry C, **113**, 6883-6886 (2009).

10. Agrawal, R., B. Peng and H.D. Espinosa, *Experimental-Computational Investigation of ZnO nanowires Strength and Fracture.* Nano Letters, **9**, 4177-4183 (2009).

11. Asthana, A. and et al., *In situ observation of size-scale effects on the mechanical properties of ZnO nanowires.* Nanotechnology, **22**, 265712 (2011).

12. Agrawal, R. and H.D. Espinosa, *Giant Piezoelectric Size Effects in Zinc Oxide and Gallium Nitride Nanowires. A First Principles Investigation.* Nano Letters, **11**, 786-790 (2011).

13. Alexe, M., S. Senz, M.A. Schubert, D. Hesse and U. Gösele, *Energy Harvesting Using Nanowires?* Advanced Materials, **20**, 4021-4026 (2008).

14. Xu, S., Y. Qin, C. Xu, Y. Wei, R. Yang and Z.L. Wang, *Self-powered nanowire devices.* Nat Nano, **5**, 366-373 (2010).

15. Momeni, K., *Experimental and theoretical study of microstructure effect on piezoelectric property of one dimensional ZnO nanostructures*, in *Mechanical Engineering-Engineering Mechanics*. 2011, Michigan Technological University: Houghton.

16. Xu, S., Y. Qin, C. Xu, Y. Wei, R. Yang and Z.L. Wang, *Self-powered nanowire devices.* Nat Nano, **advance online publication**, (2010).

17. Mohammadi, F., A. Khan and R.B. Cass: *Power Generation from Piezoelectric Lead Zirconate Titanate Fiber Composites*, edited by *Materials Research Society* **734**, 2003),p. D5.51.

18. Li, J.Y. and M.L. Dunn, *Micromechanics of Magnetoelectroelastic Composite Materials: Average Fields and Effective Behavior.* Journal of Intelligent Material Systems and Structures, **9**, 404-416 (1998).

19. Momeni, K., G.M. Odegard and R.S. Yassar, *Nanocomposite electrical generator based on piezoelectric zinc oxide nanowires.* Journal of Applied Physics, **108**, 114303-7 (2010).

20. Cherkaoui, M. and L. Capolungo, *Atomistic and continuum modeling of nanocrystalline materials : deformation mechanisms and scale transition*. Springer series in materials science. 2008, New York ; London: Springer.

21. Hull, D. and T.W. Clyne, *An introduction to composite materials*. 2nd ed. ed. 1996, Cambridge: Cambridge University Press. xvi,326p.

22. Gao, Y. and Z.L. Wang, *Electrostatic Potential in a Bent Piezoelectric Nanowire. The Fundamental Theory of Nanogenerator and Nanopiezotronics.* Nano Letters, **7**, 2499-2505 (2007).

23. Cox, H.L., *The elasticity and strength of paper and other fibrous materials.* British Journal of Applied Physics, 72 (1952).

24. Gao, X.L. and K. Li, *A shear-lag model for carbon nanotube-reinforced polymer composites.* International Journal of Solids and Structures, **42**, 1649-1667 (2005).

25. Momeni, K. and R.S. Yassar, *Analytical Formulation of Stress Distribution in Cellulose Nanocomposites.* Journal of Computational and Theoretical Nanoscience, **6**, 1511-1518 (2009).

26. Nye, J.F., *Physical Properties of Crystals*. 1957, London: Oxford.

27. Callister, W.D., *Materials science and engineering : an introduction*. 6th ed. 2003, New York: Wiley. xxi, 820 p.

28. Schubert, M.A., S. Senz, M. Alexe, D. Hesse and U. Gosele, *Finite element method calculations of ZnO nanowires for nanogenerators.* Applied Physics Letters, **92**, 122904-3 (2008).

29. Ashkenov, N., B.N. Mbenkum, C. Bundesmann, V. Riede, M. Lorenz, D. Spemann, E.M. Kaidashev, A. Kasic, M. Schubert, M. Grundmann, G. Wagner, H. Neumann, V. Darakchieva, H. Arwin and B. Monemar, *Infrared dielectric functions and phonon modes of high-quality ZnO films.* Journal of Applied Physics, **93**, 126-133 (2003).

30. Carlotti, G., G. Socino, A. Petri and E. Verona, *Acoustic investigation of the elastic properties of ZnO films.* Applied Physics Letters, **51**, 1889-1891 (1987).

31. Desai, A.V. and M.A. Haque, *Influence of electromechanical boundary conditions on elasticity of zinc oxide nanowires.* Applied Physics Letters, **91**, 183106-3 (2007).

32. Zhu, L. and X. Zheng, *Modification of the elastic properties of nanostructures with surface charges in applied electric fields.* European Journal of Mechanics - A/Solids, **29**, 337-347 (2010).